Alternative implementation of a porous media model for simulating drying of heated concrete

Benedikt Weber[1]
[1]Empa, Swiss Federal Laboratories for Material Science and Technology, Dübendorf, Switzerland

Introduction

When concrete is subjected to high temperature, capillary water evaporates and chemically bound water is released due to dehydration. This results in an increase of pore pressure, which is believed to be one of the mechanisms leading to spalling. Spalling of concrete is of high concern for the fire safety of concrete structures.

In a previous publication [1], a porous media model for simulating the pressure development in heated concrete has been presented, which is based on the classical formulation given in [2]. However, the original formulation is only valid as long as liquid water is present and as long as the temperature stays below the critical temperature (374°C). These limitations are dictated by two implementational details. The classical formulation takes the capillary pressure as a primary variable and it uses the vapor saturation pressure to eliminate the vapor pressure variable. However, both the capillary pressure and the vapor saturation pressure have a physical meaning only if the liquid saturation is not zero and the temperature is below the critical temperature. The classical formulation uses some workarounds to produce plausible results outside of the valid domain [3].

In this paper, we use a different approach, proposed by Datta [4] and already implemented by the author for gypsum [5]. Instead of strictly enforcing the equilibrium vapor pressure, the evaporation is modelled as a vapor source, which reestablishes the thermodynamic equilibrium. The same idea is also used in some drying models in the COMSOL Model Library and is called non-equilibrium formulation.

Governing Equations

Concrete is modelled as a porous material where the voids of the solid skeleton are filled with liquid and gas. The gas phase is considered a mixture of dry air and water vapor. The model is formulated as a coupled system of partial differential equations that describe the mass and energy conservation.

Conservation equations

The mass of the gaseous mixture is described by the partial densities of air and vapor, denoted as ρ_a and ρ_v, respectively. Conservation of dry air reads

$$\frac{\partial}{\partial t}(\phi(1-S)\rho_a)+\nabla\cdot\left(\rho_a\mathbf{v}_a\right)=0 \tag{1}$$

where ϕ is the porosity and S is the liquid saturation. Similarly, conservation of vapor is written as

$$\frac{\partial}{\partial t}(\phi(1-S)\rho_v)+\nabla\cdot\left(\rho_v\mathbf{v}_v\right)=\dot{m}_{\text{evap}}+\dot{m}_{\text{dehyd}} \tag{2}$$

where $\dot{m}_{\text{dehyd}}$ and $\dot{m}_{\text{evap}}$ are mass sources due to evaporation and dehydration. Conservation of liquid is written as

$$\frac{\partial}{\partial t}\left(\phi S\rho_l\right)+\nabla\cdot\left(\rho_l\mathbf{v}_l\right)=-\dot{m}_{\text{evap}} \tag{3}$$

These three conservation equations can be combined in different ways and associated with different primary variables (dependent variables in COMSOL) to obtain various formulations as detailed below.

Conservation of energy is written in the standard form:

$$\begin{aligned}\rho c_p\frac{\partial T}{\partial t}&+\nabla\cdot(-k_{\text{eff}}\nabla T)\\&+(\rho_v c_{pv}\mathbf{v}_v+\rho_a c_{pa}\mathbf{v}_a)\cdot\nabla T\\&=-\dot{m}_{\text{dehyd}}\Delta h_{\text{dehyd}}-\dot{m}_{\text{evap}}\Delta h_{\text{evap}}\end{aligned} \tag{4}$$

where Δh_{dehyd} and Δh_{evap} are the enthalpies related to dehydration and evaporation, respectively. This form is used in both the classical and the alternative implementation.

Capillary pressure

As in most porous media, capillary effects play an important role in concrete. Due to surface tension in the curved gas-liquid interface (meniscus), there is a pressure difference between the gas pressure p_g and the liquid pressure p_l. This pressure difference is called capillary pressure and is defined as

$$p_c=p_g-p_l \tag{5}$$

The capillary pressure is directly related to the liquid saturation, where the relationship is determined by the pore structure and is a characteristic of the porous medium. For a given porous material, we can find the liquid saturation from sorption experiments. Both the classical and the alternative formulation use the van Genuchten formula [6] written in the form given in [7] for ambient temperature:

$$S = \left[1 + \left(\frac{p_c^{amb}}{a} \right)^{\frac{b}{b-1}} \right]^{-1/b} \tag{6}$$

where a and b are material parameters. Reference [7] provides typical values for concrete. Most sorption isotherms found in the literature are related to ambient temperature. For higher temperatures, only few data are available and only for temperatures up to 80°C. A theoretical approach is found by considering the capillary pressure in a single tube of radius r:

$$p_c = \frac{2\sigma \cos\theta}{r} \tag{7}$$

Assuming the wetting angle θ does not change, the capillary pressure is proportional to the surface tension σ, which is a function of temperature. Additionally, the pore radius increases with increasing dehydration. The classical formulation uses the following relationship [2]

$$p_c = p_c^{amb} \left(\frac{T_{cr} - T}{T_{cr} - T_{amb}} \right)^N f_{pore}(T) \tag{8}$$

where T_{cr} is the critical temperature (374°C) and N is a value close to one. The term in parentheses is one at ambient temperature and zero at the critical temperature, at which point the surface tension disappears and the capillary pressure has no physical meaning anymore. The function $f_{pore}(T)$ considers the effect of increasing pore radius with dehydration. Sorption isotherms for different temperatures are shown in Figure 1.

The capillary pressure also determines the equilibrium vapor pressure, defined as the vapor saturation pressure above a curved liquid-vapor interface. This equilibrium pressure is described by the Kelvin equation:

$$p_v^{eq} = p_{sat}(T) \cdot \exp\left(\frac{-p_c M_w}{\rho_l R T} \right) \tag{9}$$

The relations given in Eqs. (5) and (9) together with the sorption isotherms are the main equations connecting the pressures of the liquid and the gas phase in the porous medium.

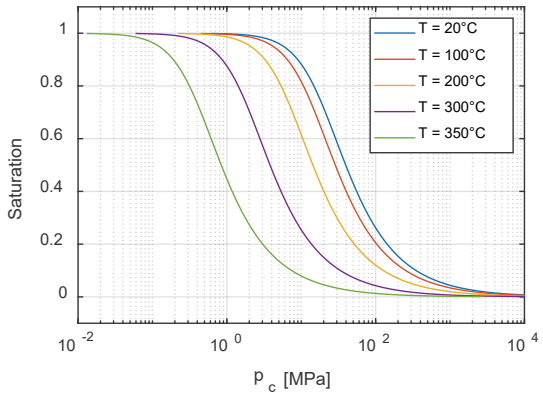

Figure 1. Saturation vs. capillary pressure.

Mathematical Model

Combining the mass conservation equations together with the capillary pressure relations in different ways and using different primary variables leads to various mathematical formulations. Traditionally, a unique, classical formulation has been used in most models for heat and mass transfer in concrete [2]. Nevertheless, other formulations are commonly used in other fields such as food processing [4] or in ground water flow and petroleum industry [8].

There is a certain freedom in selecting the primary variables and combining them with the governing equations. However, certain choices will lead to better conditioning of the system of equations than others. In addition, boundary conditions are also affected. Note that essential (Dirichlet) boundary conditions are related to the primary variables, whereas natural (Neumann) boundary conditions are related to the flux term in the equations. We first briefly recall the classical formulation and then describe an alternative model for drying of concrete at high temperature in more detail.

Classical formulation

In the classical formulation, conservation of air (1) is used unchanged. The natural primary variable would be the air pressure. However, to prescribe the ambient pressure as a Dirichlet boundary condition, the gas pressure is better suited as primary variable.

Equations (2) and (3) are combined to a conservation equation of water species. The advantage of combining liquid and vapor conservation is that the evaporation mass is removed from the global system of equations. Once the primary variables are solved, it can be recovered from the vapor conservation equation (2). The boundary condition is a mass flux

boundary condition for the water species. The vapor flux is usually specified with a mass transfer coefficient whereas the liquid flux is neglected. For the primary variable, the classical formulation uses the capillary pressure.

The two mass conservation equations are solved for the primary variables gas pressure and capillary pressure. Using Eq. (5), these two variables also define the liquid pressure. Hence, the pressures of both phases are known. The saturation is calculated from Eq. (6) where the influence of temperature is considered by Eq. (8). What is missing is the partial pressure of water vapor. The vapor pressure is assumed to be equal to the vapor saturation pressure, which is a function of temperature and capillary pressure [Eq. (9)].

If no water is present or if the temperature is above the critical temperature of water, neither the vapor saturation pressure nor the capillary pressure have a physical meaning. The classical formulation makes thus no physical sense when the saturation is zero or when the temperature goes above the critical temperature. However, it is possible to extend the numerical model formally to these situations [2,3].

Alternative model

To overcome the drawbacks of the classical formulation, we propose here an alternative model. The conservation equations for air and vapor are combined to a conservation equation for gas. For ideal gases, the partial densities for air and vapor add up to the gas density:

$$\rho_g = \rho_a + \rho_v \tag{10}$$

Adding Eqs. (1) and (2) yields a conservation equation for the gas mixture:

$$\frac{\partial}{\partial t}(\phi(1-S)\rho_g) + \nabla\cdot\left(\rho_g \mathbf{v}_g\right) = \dot{m}_{\text{evap}} + \dot{m}_{\text{dehyd}} \tag{11}$$

The gas velocity is expressed in terms of the gas pressure by Darcy's law

$$\mathbf{v}_g = -\frac{\kappa_{rg} K}{\mu_g}\nabla p_g \tag{12}$$

where K is the intrinsic permeability, κ_{rg} is the relative gas permeability, which depends on saturation, and μ_g is the dynamic viscosity. Assuming ideal gases, the gas density can be described by the gas pressure:

$$\rho_g = \frac{p_g M_g}{RT} \tag{13}$$

where M_g is the molar mass of the gas mixture and R is the universal gas constant. All quantities in Eq. (11) depend thus on the gas pressure, which is a natural candidate for the primary variable. As discussed for the classical formulation, this variable is also suitable to formulate a pressure boundary condition.

In the alternative model, the relative amounts of air and vapor in the gas phase are described by the primary variable of mass fraction

$$\omega_v = \rho_v / \rho_g \tag{14}$$

Combining Eqs. (1) and (2), and substituting Eq. (11) yields [5]

$$\begin{aligned}\phi(1-S)\rho_g \frac{\partial \omega_v}{\partial t} + \rho_g \mathbf{v}_g \cdot \nabla\omega_v + \nabla\cdot\mathbf{j}_v \\ = (1-\omega_v)(\dot{m}_{\text{dehyd}} + \dot{m}_{\text{evap}})\end{aligned} \tag{15}$$

The diffusive flux is governed by Fick's law. It depends directly on the mass fraction:

$$\mathbf{j}_v = -\rho_g D_{eff}\nabla\omega_v \tag{16}$$

where D_{eff} is the effective diffusion coefficient. The mass fraction is also suitable for the flux boundary condition. Instead of prescribing the vapor mass flux as in the classical formulation, we use an outflow boundary condition. Employing the natural boundary condition $\mathbf{j}_v = 0$, the air-vapor mixture leaves the concrete according to the gas pressure without changing its composition. This boundary condition, which is independent of the ambient humidity, makes sense since we know that a positive gas pressure develops due to heating.

In the alternative formulation, the liquid conservation equation (3) is used unchanged. The liquid velocity is described by Darcy's law

$$\mathbf{v}_l = -\frac{\kappa_{rl} K}{\mu_l}\nabla p_l \tag{17}$$

where the liquid pressure is found via the capillary pressure [Eq. (5)], which depends on saturation. Liquid water is assumed incompressible and the liquid pressure is hence not suitable as primary variable. A natural choice for describing the water content is the saturation, which is taken as primary variable. For the liquid boundary condition, an outflow condition proposed by Lenzinger and Schweizer [9] is used:

$$-\mathbf{n}\cdot(\rho_l \mathbf{v}_l) = -K_0^l \left\langle p_l - p_g^{amb} \right\rangle^+ \tag{18}$$

where K_0^l is a large constant and $\langle . \rangle^+$ denotes the positive part. The idea behind this boundary condition is that the capillary pressure vanishes at the boundary and the liquid water moves out quickly as long as the liquid pressure is less than the ambient gas pressure.

The capillary pressure is determined from the liquid saturation and the temperature. First, the value corresponding to ambient temperature is calculated from the inverse of Eq. (6):

$$p_c^{amb} = a\left(S^{-b} - 1\right)^{(1-1/b)} \tag{19}$$

The capillary pressure at temperature T is then determined by Eq. (8). In this formulation, it is assumed that no liquid water is present beyond the critical temperature and the capillary pressure is not used in this temperature region.

For the relative gas permeability in Eq. (12) most models use the formula derived by van Genuchten from the sorption isotherms [6]:

$$\kappa_{rg} = \sqrt{1-S}\left(1-S^b\right)^{2/b} \tag{20}$$

The corresponding liquid permeability is given by

$$\kappa_{rl} = \sqrt{S}\left[1-\left(1-S^b\right)^{1/b}\right]^2 \tag{21}$$

where b is the same parameter as in Eq. (19).

In the classical formulation, only two mass conservation equations are used to solve for two primary variables. A third equation, the vapor conservation equation, is used to find the evaporation mass. In the alternative formulation, on the other hand, all three mass conservation equations are used to solve for three primary variables. The evaporation mass has thus to be found by some other means. It is calculated from the deviation of the vapor pressure from equilibrium:

$$\dot{m}_{evap} = K_0^{evap}\frac{M_w}{RT}\left(p_v^{eq} - p_v\right) \tag{22}$$

Because the vapor pressure equilibrium is not strictly enforced, this formulation is also called non-equilibrium formulation [4]. Eq. (22) can be considered either as modelling the actual evaporation rate or as a penalty formulation enforcing the vapor pressure equilibrium approximately. Taking the latter interpretation, the constant K_0^{evap} is just a number, large enough to make the deviation from equilibrium small, but limited to avoid numerical problems.

For energy conservation, the heat equation (4) is used. Boundary conditions on the heated surface are specified by heat flux by convection and radiation:

$$-\mathbf{n}\cdot(-k_{\text{eff}}\nabla T) = h_T(T_{\text{ext}} - T) + \sigma\varepsilon\left(T_{\text{ext}}^4 - T^4\right) \tag{23}$$

where h_T is the heat transfer coefficient, σ is the Stefan-Boltzmann constant and ε is the surface emissivity. For the heated surface, T_{ext} is the radiator temperature. On the cold face, only heat convection is specified, where T_{ext} is the ambient temperature.

Regularization

In contrast to the classical formulation, the saturation is not automatically restricted to the range $0 \le S \le 1$. While the upper limit is not reached in the current simulations, the lower limit has to be enforced by switching off evaporation when the saturation approaches zero. Condensation, on the other hand is still possible at zero saturation. The implementation used in the alternative model is suggested in the user's guide for the Chemical Reaction Interface. The deviation of the vapor pressure from the equilibrium vapor pressure in Eq. (22) is replaced by the following expression:

$$\Delta p_v = \underbrace{\left\langle p_v^{eq} - p_v \right\rangle^+}_{\substack{\text{positive part}\\ \text{evaporation}}} \frac{\max(S-\varepsilon_S, 0)}{\max(S-\varepsilon_S, \varepsilon_S)} + \underbrace{\left\langle p_v^{eq} - p_v \right\rangle^-}_{\substack{\text{negative part}\\ \text{condesation}}} \tag{24}$$

The positive part of the deviation corresponds to evaporation and the negative part to condensation. The positive part is reduced linearly between $S = 2\varepsilon_S$ and the threshold saturation $S = \varepsilon_s$.

Since Eq. (24) controls only the evaporation mass but not the saturation itself, the resulting saturation does not drop down to exactly zero but exhibits some numerical noise. To avoid numerical problems with small negative saturations, the saturation needs to be regularized for evaluating the capillary pressure [Eq. (19)] and the relative permeabilities [Eqs. (20) and (21)]. The regularized quantity is

$$S_{reg} = \max(S, \varepsilon_s) \tag{25}$$

The restriction posed in Eq. (24) takes care of saturations near zero but not of temperatures near the critical temperature. The problem is that the equilibrium vapor pressure p_v^{eq} is undefined at the critical temperature and cannot be used in Eq. (24). Numerically, the capillary pressure becomes small near the critical temperature, resulting in a high equilibrium vapor pressure according to Eq. (9) and thus in a high pressure difference $p_v^{eq} - p_v$ in Eq. (24). Although the corresponding evaporation mass is suppressed for saturations near zero, it can lead to instabilities when the saturation exhibits some perturbation around zero, which is typically the case. To avoid this problem, another regularization is needed that stops evaporation when the critical temperature is approached. The expression is similar to the regularization in Eq. (24). However, no distinction is made between a positive and negative part of the pressure difference, since neither

evaporation nor condensation should occur in this case:

$$\dot{m}_{evap} = K_0^{evap} \frac{M_w}{RT} \Delta p_v \frac{\max(T - T_{cr} - \varepsilon_T, 0)}{\max(T - T_{cr} - \varepsilon_T, \varepsilon_T)} \quad (26)$$

Finally, the liquid pressure is also affected by the capillary pressure. However, the saturation and the relative permeability in the liquid conservation equation (3) seem to take care of the degenerate case.

COMSOL implementation

All equations have been implemented in COMSOL Multiphysics without any additional modules. The heat and mass conservation equations were transformed into the weak form and put into the 2D Weak Form interface. Constitutive equations and material parameters were put into Definitions nodes. The standard BDF time stepping algorithm was selected.

Although some physics interfaces could have been used, it seemed advantageous to stay with the equation based interfaces for developing a new model and exploring different formulations.

Results and discussion

Experimental data

The same experimental data [10] are used as in the previous paper [1]. A concrete plate of 120 mm thickness is heated by a radiant heater placed 3 cm above the upper surface as shown in the experimental setup scheme in Figure 2. According to the reference, the temperature of the heater was 600 C°. The lateral faces of the specimen are insulated with porous ceramic blocks. The specimen contains combined temperature and pressure sensors located at different depths. The concrete was a high performance concrete made with calcareous aggregates and with a compressive strength of 100 MPa.

Although reference [10] specifies a radiator temperature of 600 C°, applying the simple boundary condition (27) leads to temperatures much larger than the measured ones. Following [3], the external temperature is specified as starting at 400 C° and increasing up to 460 °C. The intrinsic permeability is taken as $K = 5 \times 10^{-20}$ m^2. This value has been chosen by calibration of the pressure peaks.

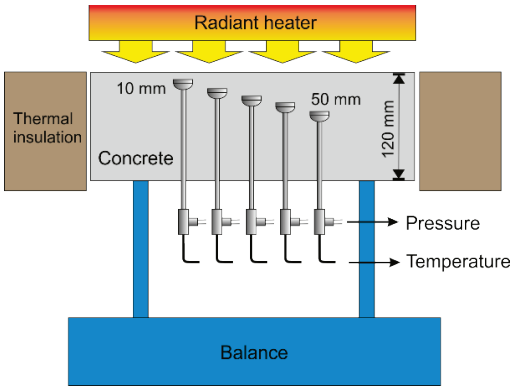

Figure 2. Experimental setup.

Discretization and computation

Since the behavior of the experiment is essentially one-dimensional, only a one row of 100 elements has been used over the thickness of the slab. To better capture the pressure profiles, an arithmetic distribution of element sizes was selected with smaller elements near the upper and lower surface. The typical computing time on an Intel i-7 processor with four cores was around 2 minutes.

Results

The comparison of the temperature fields shown in Figure 3 shows a good agreement with the experimental observations. These results are very similar to the ones obtained by the classical model.

To get a better idea of the modelling effect, selected results are shown on the next page using the classical and the alternative formulation.

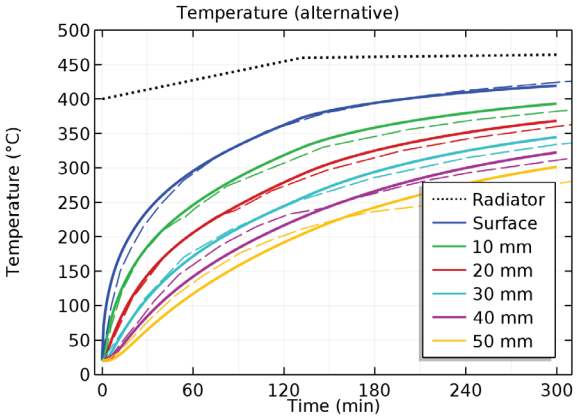

Figure 3. Comparison of temperature. (Solid lines simulations, dashed lines experimental data

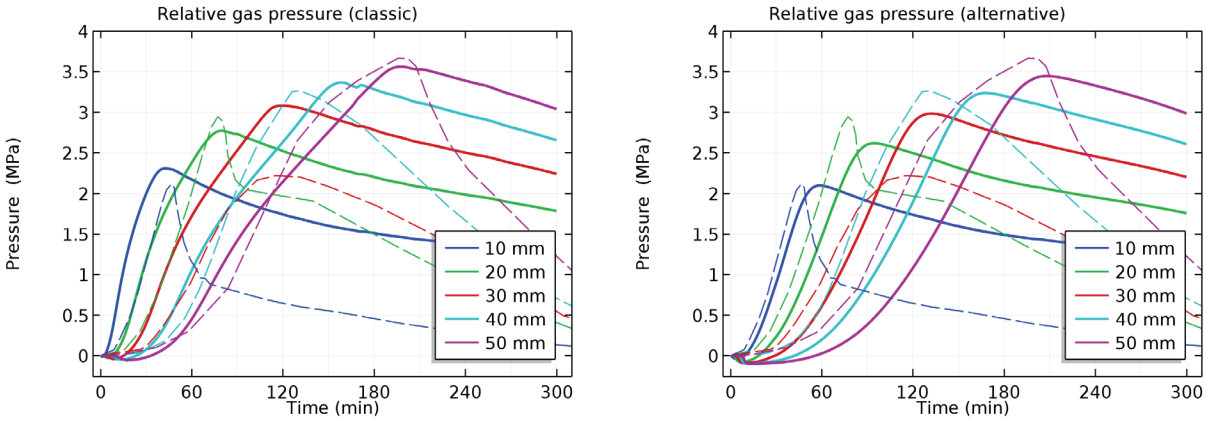

Figure 4. Comparison of simulated gas pressure (solid) with experimental data (dashed): classical formulation (left) and alternative implementation (right).

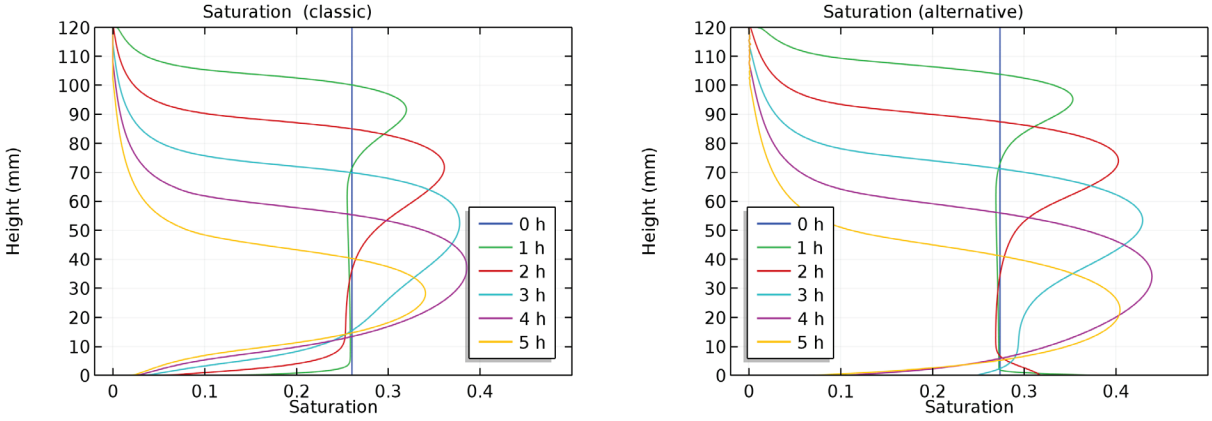

Figure 5. Comparison of simulated saturation profiles (solid) with experimental data (dashed): classical formulation (left) and alternative implementation (right).

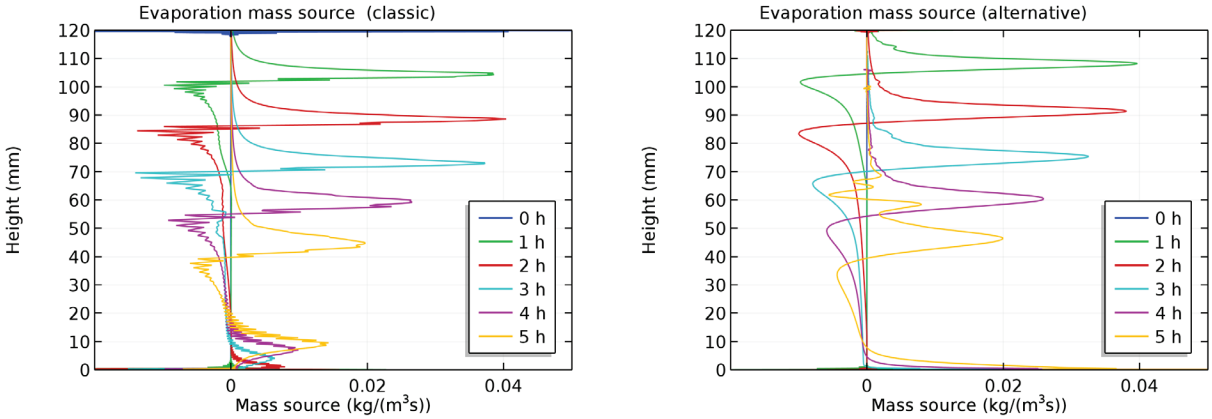

Figure 6. Comparison of simulated evaporation-mass profiles (solid) with experimental data (dashed): classical formulation (left) and alternative implementation (right).

Pressure profiles are shown in Figure 4. Pressure peaks are well captured in both implementations when the calibrated intrinsic permeability is used, although the position is a bit shifted. The alternative model better reflects the form of the pressure increase before the peaks, while both implementations show less agreement for the post peak behavior. It is believed that the pressure drop after the peaks is due to micro-cracking, which is not included in the models.

Saturation profiles obtained from the classical and the alternative formulation are shown in Figure 5. As expected, the saturation is zero at the heated to surface. The classical formulation approaches the zero value in a smooth way, whereas the alternative implementation reaches zero saturation at the depth where the critical temperature is reached (hardly visible). The different behavior at the bottom is likely due to the different flux boundary conditions.

Interesting are also the profiles of evaporation mass, shown in Figure 6. The curves look globally very similar for both models, but the classical implementation exhibits some local disturbances. These oscillations seem not to carry over to the saturation curves, which are smooth in both models. The evaporation profiles obtained by the alternative implementation show a smoother behavior.

Conclusions

In order to overcome some nonphysical details of the classical model for heated concrete, an alternative implementation has been developed. The new implementation uses a non-equilibrium formulation, where evaporation depends on the difference between actual pressure and equilibrium pressure. With this formulation, it is possible to switch to the regime where the capillary pressure and the equilibrium vapor pressure have no physical meaning and cannot be used. Using the equation-based interface in COMSOL, it is relatively easy to explore alternative conservation equations and to use different primary variables. The generalization in the new implementation comes at the cost of an additional primary variable and some regularizations that have to be implemented.

Both models are applied for simulating an experiment of heated concrete from the literature. Both provide similar results, which agree well with the experimental data. However, it should be kept in mind that the important changes in saturation and the pressure occur before the saturation reaches zero and the temperature passes the critical value. In this sense, the example is not a relevant test case. Thus, from a practical point of view, the extra effort of the alternative implementation may be questioned. Nevertheless, the new model is believed to be more transparent concerning the underlying physics.

References

1. B. Weber, D. Dauti, and S. Dal Pont, COMSOL Implementation of a porous media model for simulating pressure development in heated concrete, *Comsol Conference,* Munich (2016).
2. D. Gawin, F. Pesavento, and B. Schrefler, What physical phenomena can be neglected when modelling concrete at high temperature? A comparative study. Part 1: Physical phenomena and mathematical model, *International Journal of Solids and Structures* **48,** 1927–1944 (2011).
3. D. Gawin, F. Pesavento, and B. Schrefler, Modelling of hygro-thermal behaviour and damage of concrete at temperature above the critical point of water, *International Journal for Numerical and Analytical Methods in Geomechanics*, **26**, 537–562 (2002).
4. A.K. Datta, Porous media approaches to studying simultaneous heat and mass transfer in food processes. I: Problem formulations, *Journal of Food* Engineering **80,** 80–95 (2007).
5. B. Weber, Heat transfer mechanisms and models for a gypsum board exposed to fire, *International Journal of Heat and Mass Transfer* **55,** 1661–1678 (2012).
6. M.T. van Genuchten, A closed-form equation for predicting the hydraulic conductivity of unsaturated soils. *Soil Sci Soc Am J,* **44**, 892–8 (1980).
7. V. Baroghel-Bouny, M. Mainguy, T. Lassabatere, O. Coussy, Characterization and identification of equilibrium and transfer moisture properties for ordinary and high-performance cementitious materials, *Cement and concrete research*, **29**, 1225–1238 (1999).
8. Z. Chen, G. Huan, and Y. Ma, *Computational methods* for *multiphase flows in porous media,* Siam (2006).
9. M. Lenzinger, B. Schweizer, Two-phase flow equations with outflow boundary conditions in the hydrophobic-hydrophilic case, *Nonlinear Analys.* **73**, 840–853 (2010).
10. P. Kalifa, F.-D. Menneteau, and D. Quenard, Spalling and pore pressure in HPC at high temperatures, *Cement and concrete research*, **30**, 1915–1927 (2000).